Dihapto Arene Binding at High-Spin Fe(I) Enabled by a Sterically Accommodating Tris(pyrazolyl)hydroborate Ligand

Laura A. Essex,[†] Alex McSkimming,[†] Niklas B. Thompson,[§] Margaret L. Kelty,[‡] Ethan A. Hill,[‡] and W. Hill Harman[†,*]

[†]*Department of Chemistry, University of California, Riverside, CA 92521*

[§]*Massachusetts Institute of Technology, 32 Vassar St. Cambridge MA 02139*

[‡]*University of Chicago, 5735 S Ellis Ave. Chicago IL 60637*

ABSTRACT: Transition metal arene complexes are important species in catalysis and arene functionalization. Certain electron rich metal fragments are capable of binding arenes across two adjacent carbon atoms, inducing significant dearomatization through strong backbonding interactions. Such complexes generally adopt low-spin, closed-shell configurations with electronic and coordinative saturation. Herein, we report an asymmetric trispyrazolylhydroborate (Tp) ligand and its Fe(I) fragment, which forms dihapto complexes with a range of arenes and heteroarenes including benzene, trifluoromethylbenzene, naphthalene, anthracene, and furan. X-band EPR and solution magnetometry definitively establish these complexes as high spin (S = 3/2), owing to the relatively weak ligand field provided by Tp. These compounds expand a small but growing family of complexes that feature strongly backbonding metal fragments in high-spin configurations.

INTRODUCTION

Arenes are an important class of ligands in organometallic chemistry,[1] serving as spectator ligands or substrates in the functionalization of the arene itself. The hapticity of unsupported arene ligands is determined by the electronic properties of the metal center to which it is bound, according to the 18-electron rule and related concepts. If sterically accessible, η^6 binding is the norm, as it preserves the aromaticity of the arene. With electron-deficient metal fragments, hexahapto coordination can imbue reactivity with nucleophiles (e.g. group 6 $(CO)_3M$(arene) complexes).[2] In some cases, ring-slippage to tetrahapto coordination occurs, as in the reduction of $[(\eta^6\text{-}C_6Me_6)_2Ru]^{2+}$ to $(\eta^6\text{-}C_6Me_6)Ru(\eta^4\text{-}C_6Me_6)$.[3] With some metal fragments, dihapto binding of arenes is observed,[4] and in the case of electron-rich, π-basic metal fragments, the metal-arene interaction is driven by strong backbonding (Chart 1). This transfer of electron density into the arene π* orbitals perturbs the aromaticity of the ring system and can drive reactivity of the bound arene with electrophiles.[5] Owing to the use of strong-field ligands and/or second- and third-row metals, the η^2-arene complexes reported to date tend to be electronically saturated and low-spin. We have been interested in the chemistry of low-valent Fe fragments supported by trispyrazoylhydroborate (Tp) ligands,[6] which, in the Fe(I) state, bind unsaturated ligands (e.g. N_2[7] and CO[8]) with strong activation of the substrate via backbonding. Crucially, the metal centers in these complexes populate a high-spin (S = 3/2) ground state despite the coordination of a π-accepting substrate. Low-coordinate TpFe complexes can be prepared with bulky Tp ligands of the "tetrahedral enforcer" variety,[9] and their sterically encumbered Fe centers limit the size of accessible fourth ligands. Herein we report the development of a new Tp scaffold which, while bulky enough to allow the preparation of low-coordinate TpFe(I) complexes, contains an open face due to a regiochemical switch where one of the larger substituents is oriented away from the apical pocket This steric accommodation allows for the access of larger ligands to the metal center. Using this weak-field Fe(I) fragment, we have prepared the first examples of high-spin, η^2-arene/heteroarene adducts and definitively established their spin state via EPR and solution magnetometry.

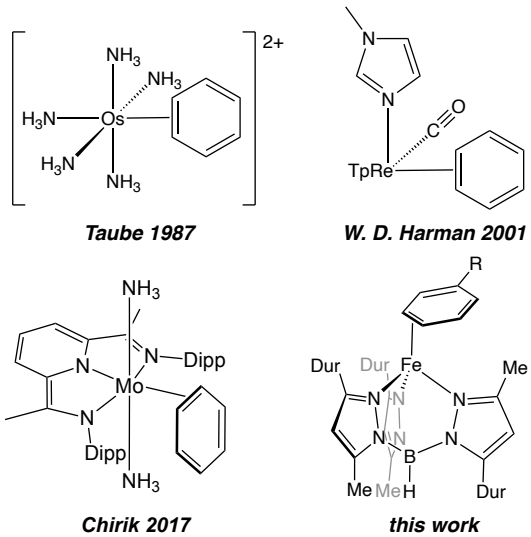

Chart 1. A selection of mononuclear η^2-arene complexes of π-basic transition metal fragments (Dur = 2,3,5,6-tetramethylphenyl, Dipp = 2,6-diisopropylphenyl).

RESULTS AND DISCUSSION

After discovering that sufficiently bulky Tp ligands could enable access to an unprecedented mononuclear S = 3/2 Fe(I) complex of N_2,[7a] we began to explore other Tp variants in order

to find supporting ligands that were less sterically imposing but still capable of supporting low-coordinate, monometallic Fe(I) centers. To this end, we synthesized a Tp ligand derived from 5-methyl-3-duryl-1H-pyrazole (**2**, duryl = Dur = 2,3,5,6-tetramethylphenyl). After subjecting **2** to standard Tp synthesis conditions with $NaBH_4$, we isolated a single product whose ^1H NMR spectrum was inconsistent with a threefold symmetric Tp scaffold (Scheme 1, Figure S1). Instead, the solution ^1H features two different sets of pyrazole resonances in a 2:1 ratio, consistent with an inversion of the regiochemistry of the B–N bond forming step for one of the pyrazoles to give sodium bis(5-methyl-3-(2,3,5,6-tetramethylphenyl)-1-pyrazolyl)(3-methyl-5-(2,3,5,6-tetramethylphenyl)-1-pyrazolyl)hydroborate ($NaTp^{Me,Dur}$, **3**) in 56% yield. This regiochemistry has been observed in other Tp derivatives and is presumably a consequence of very bulky aryl substituents at the 3-position of the pyrazole.[10] Compound **3** is noteworthy, however, for the relative ease of its synthesis compared to other Tp ligands with similar regiochemistry, which tend to be produced as a mixture of isomers.

Scheme 1. Synthesis of $[Tp^{Dur,Me}]^-$ and Its Iron Complexes

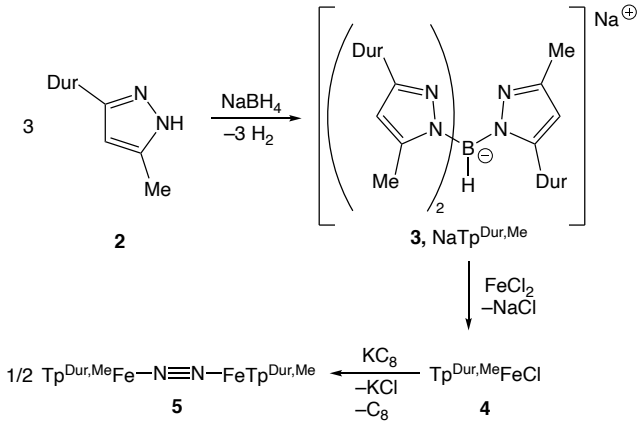

Tp ligand **3** could be metallated with iron(II) chloride to give the paramagnetic complex $Tp^{Me,Dur}FeCl$ (**4**, Scheme 1). Single-crystal X-ray diffraction (XRD) confirmed this structural assignment and the unusual regiochemistry of **3**, revealing a pseudotetrahedral Fe(II) center flanked by two duryl substituents and a methyl group (Figure 1). A single, irreversible reduction event was observed for **4** at $E_{p,c}$ = –2.97 V vs. Fc/Fc^+ by cyclic voltammetry in THF (Figure S26) indicating the plausibility of accessing formally Fe(I) complexes with this framework. To wit, reduction of **4** with KC_8 affords the formally Fe(I) N_2 complex $(Tp^{Me,Dur}Fe)_2(\mu\text{-}N_2)$ (**5**, Scheme 1), which, despite the significant steric bulk presented by the duryl substituents, was shown to exist as a bimetallic complex with a bridging N_2 ligand in the solid state by XRD (Figure 1, bottom). While complex **5** is structurally analogous to the complex $(Tp^{Ph,Me}Fe)_2(\mu\text{-}N_2)$ previously reported by our group,[7a] the phenyl-substituted analogue exhibits nearly perfect threefold symmetry due to the interdigitation of the phenyl substituents. In contrast, the TpFe units in **5** are strongly canted away from the latent threefold axis, with the methyl group, due to its smaller size, encroaching on the bridging N_2 ligand. Complex **5** is dark red both in the solid state and in THF solution. Like its phenyl-substituted analogue, **5** exhibits an intense band at 910 nm in the UV-vis-NIR spectrum, consistent with an intact Fe–N_2–Fe unit in solution.[7a,11] Unlike its phenyl congener, however, **5** undergoes an immediate and reversible color change to black when dissolved in benzene under N_2, accompanied by the disappearance of the NIR feature characteristic of the Fe–N_2–Fe unit. Working under argon allows the isolation of this material as a black microcrystalline solid. Despite significant effort, we have been unable to generate single crystals suitable for its structural characterization via XRD. Vibrational spectroscopy provided no indication of a bound N_2 ligand, and combustion analysis is consistent with the formulation of this complex as the benzene adduct $Tp^{Dur,Me}Fe(C_6H_6)$ (**6**). Solution magnetometry conducted on **6** by the method of Evans[12] gave an effective magnetic moment of 3.9 ± 0.1 μ_B, consistent with a high-spin, monometallic Fe(I) complex. In further support of the high-spin assignment, the X-band EPR spectrum of **6** in 2-methyltetrahydrofuran (2-MeTHF) at 109 K contained a broad feature spanning ~0–500 mT (Figure S20), inconsistent with an S = ½ complex. Given the rarity of arene complexes featuring high-spin metal centers, we were eager to gain more information on this class of molecules and so turned to alternate arene ligands in order to identify related complexes amenable to structural characterization.

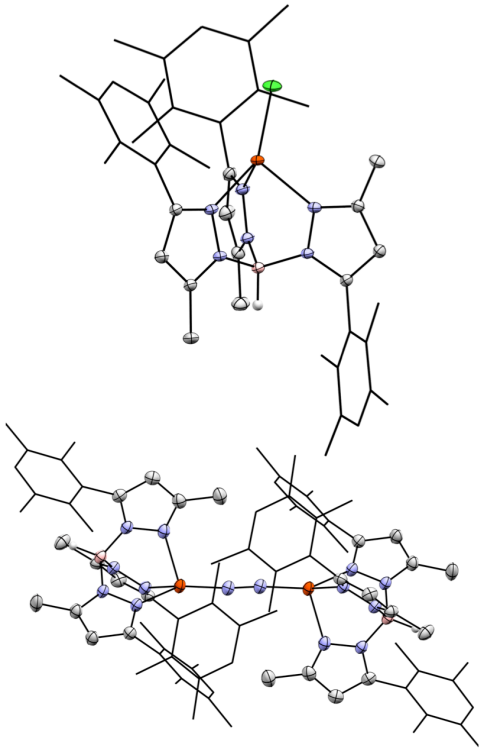

Figure 1. Thermal ellipsoid plots (50% probability) of the solid-state structure of $Tp^{Me,Dur}FeCl$ (**4**, top) and $(Tp^{Me,Dur}Fe)_2(\mu\text{-}N_2)$ (**5**, bottom). Orange, blue, pink, and gray ellipsoids represent Fe, N, B, and C atoms, respectively. Most hydrogen atoms and co-crystallized solvent molecules are omitted for clarity.

Due to its electron deficient character, $PhCF_3$ has been used as a benzene surrogate in systems that bind arenes in a dihapto fashion,[13] with an ~3 kcal/mol greater binding energy reported for a Mo(0) system.[14] Dissolution of **5** in $PhCF_3$ under argon resulted in the quantitative formation of a new purple species (Scheme 2) with a solution magnetic moment (μ_{eff} = 3.9 ± 0.1 μ_B) and optical properties (Figure S16) similar to those of **6**. Slow evaporation of a pentane solution of this material gave single crystals which were shown by XRD to be the dihapto arene complex $Tp^{Dur,Me}Fe(3,4\text{-}\eta^2\text{-}PhCF_3)$ (**7**, Figure 2). Compound **7** is the first example of a crystallographically characterized η^2-$PhCF_3$ complex, and its solid-state structure contains

two crystallographically independent but chemically equivalent molecules with minor variations in bond distances. The coordinated π bond is elongated significantly (d_{C-C} = 1.427(4), 1.428(4) Å) compared to free $PhCF_3$,[15] and the uncoordinated portion of the arene exhibits bond lengths consistent with perturbation of the aromaticity of the bound ligand (Figure 2, right). Inspection of a space-filling model of **7** suggests that the open face of the $Tp^{Dur,Me}$ ligand with the flanking methyl group is critical for accommodating arene binding to this otherwise sterically bulky fragment.

Scheme 2. Synthesis of $Tp^{Dur,Me}Fe(I)$ Arene Complexes

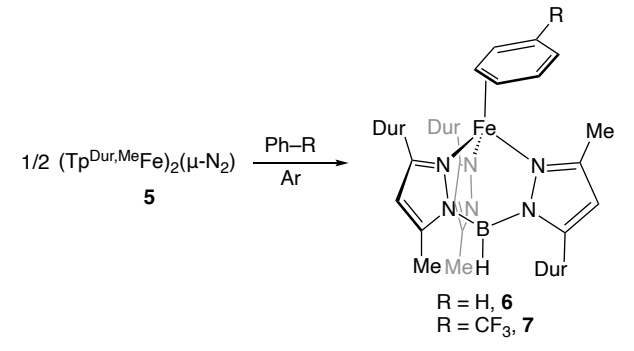

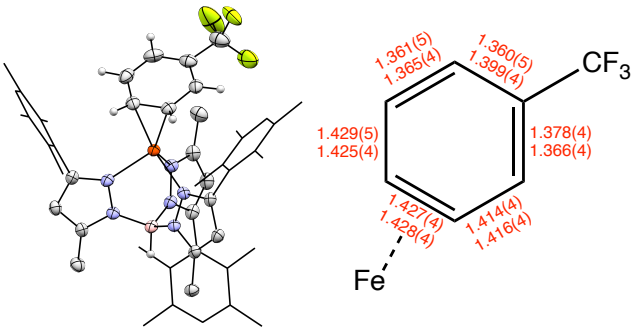

Figure 2. Thermal ellipsoid plot (50% probability) of one of independent molecules in the solid-state structure of $Tp^{Me,Dur}(3,4\text{-}\eta^2\text{-}PhCF_3)$ (**7**, left) and selected bond lengths for both independent molecules (right). Bond lengths are given in Å. Orange, blue, pink, and gray ellipsoids represent Fe, N, B, and C atoms, respectively. One disordered CF_3 group, co-crystallized solvent molecules, and most hydrogen atoms have been omitted for clarity.

Having confirmed the structure of **7** via single crystal XRD, we were eager to definitively establish its spin-state. Like complex **6**, the X-band EPR spectrum of **7** at 105 K is extremely broad (Figure S19). However, a sample of **7** in hexane cooled to 15 K exhibits a well-resolved spectrum with features at apparent g values (g_{eff}) of 5.8, 2.3, and 1.7, consistent with rhombic S = 3/2 complex ($E/D \approx 0.3$) with $g_{iso} > 2$ (Figure 3).[16] The ^{57}Fe Mossbauer spectrum of **7** contains a quadrupole doublet with an isomer shift of 0.951 mm/s and a quadrupole splitting of 1.011 mm/s. (Figure S24). Although Mössbauer data on low-coordinate TpFe complexes are scant, the large isomer shift is consistent with a high-spin assignment.[17]

Density functional theory (DFT) calculations of the model complex $TpFe(3,4\text{-}\eta^2\text{-}PhCF_3)$ were carried out on both the doublet and quartet manifolds in order to gain further insight into the electronic structure of **7** (M06L[18] with a custom Alrichs basis[19] set via ORCA,[20] see SI). Although energy minima featuring dihapto arene coordination could be converged in both spin states (Figures S33 and S34), the S = 3/2 configuration was significantly lower in energy (ΔE = 0.0389 E_h) and better reproduced the longer Fe–N and Fe–C bond lengths observed by XRD. A spin density plot generated for the high-spin structure of $TpFe(3,4\text{-}\eta^2\text{-}PhCF_3)$ (Figure 4) shows significant spin delocalization onto the bound arene, with Mulliken spin populations of 3.33 at Fe and –0.13 on each of the two bound carbons. We observed a similar phenomenon in our computational investigation of the related terminal N_2 complex $Tp^{Ad,Me}Fe(N_2)$,[7a] and this spin polarization may be a key difference between π-basic fragments with weak ligand fields and more typical strong-field π-bases.[21]

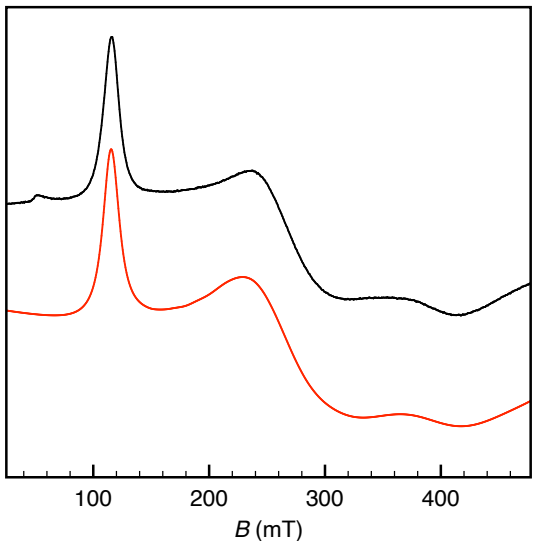

Figure 3. X-band EPR spectrum (9.631 GHz) of $Tp^{Me,Dur}Fe(3,4\text{-}\eta^2\text{-}PhCF_3)$ in hexane at 15 K (black) and its simulation (red) with the following parameters: g = [2.4, 2.2, 2.2], E/D = 0.31. See Supporting Information for simulation details.

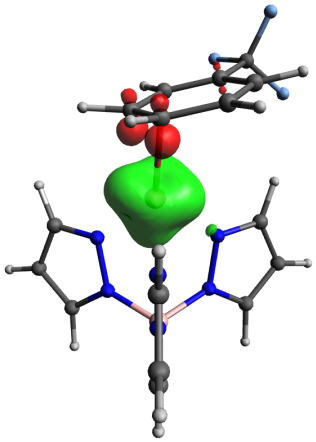

Figure 4. Spin-density isosurface (0.01) calculated for the model high-spin complex $TpFe(\eta^2\text{-}PhCF_3)$. Green represents positive spin and red represents negative spin. Mulliken spin populations: Fe = 3.33, C1 = −0.13, C2 = −0.13.

Having established that **7** is a bona fide high-spin Fe(I) complex of a dihapto arene, we explored the generality of this motif. Treatment of **5** with naphthalene, anthracene, and furan under Ar gave rise to isolable complexes of the form $Tp^{Dur,Me}Fe(\eta^2\text{-}L)$

(Scheme 3) where L = naphthalene (**8**), anthracene (**9**), and furan (**10**). Complex **8** can also be synthesized directly from **4** via reduction with $K(C_{10}H_8)$. Like **7**, compounds **8**–**10** are also S = 3/2, with solution magnetic moments ranging from 3.7–3.9 μ_B and broad X-band EPR spectra spanning hundreds of mT (Figures S21–23). Single crystal XRD confirms the dihapto ligand binding in **8**–**10** (Figure 5). These structures feature lengthening of the coordinated C–C bond (d_{C-C} > 1.4 Å) consistent with significant backbonding, and **10** is a rare example of a structurally characterized mononuclear η^2-furan complex.[22] Although complexes **6** and **7** slowly reform the bridging N_2 complex **5** in the presence of N_2, **8** and **9** are indefinitely stable in ethereal solvents under the same conditions. The furan complex **10**, however, cannot be prepared except by the rigorous exclusion of N_2, and we observed no binding between the $Tp^{Dur,Me}Fe(I)$ fragment and N-methylpyrrole. These findings are consistent both with the diminished aromaticity of naphthalene and anthracene relative to benzene as well as the centrality of backbonding to these interactions, weakening the ability of the electron-rich substrates furan and N-methylpyrrole to coordinate.

Scheme 3. Synthesis of Polycylic Arene and Heteroarene Complexes of $Tp^{Dur,Me}Fe(I)$

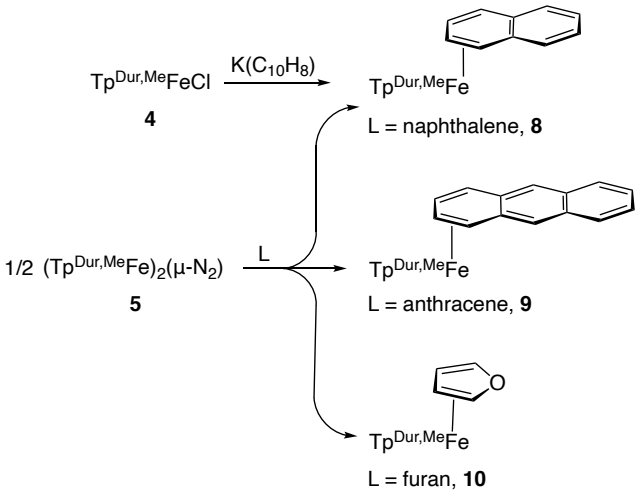

CONCLUSIONS

We have developed a new, readily synthesized Tp ligand which is bulky enough to support low-coordinate Fe(I) complexes while preserving a binding site that can accommodate large unsaturated ligands. This fragment binds a range of arenes and heteroarenes to give dihapto complexes that populate a high-spin (S = 3/2) ground state. These compounds are unusual given the plethora of low-spin Fe(I) complexes featuring hexahapto arene coordination[11,23] and the lack of high-spin dihapto arene complexes. DFT calculations suggest the delocalization of unpaired spin onto the bound arene, and, given the utility of dihapto coordination in the functionalization of arenes with electrophiles, we are currently exploring analogous chemistry, with a focus on radical-mediated processes.

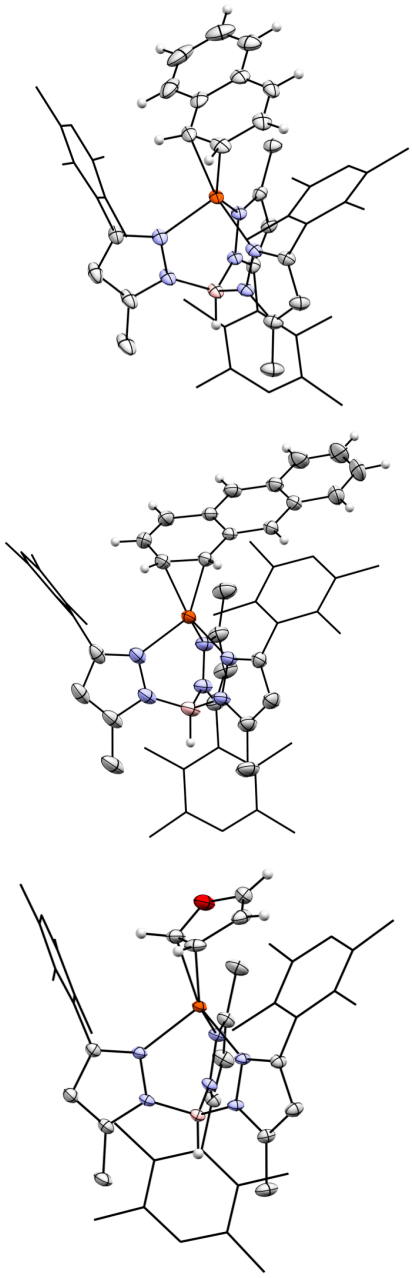

Figure 5. Thermal ellipsoid plots (50% probability) of the solid-state structures of $Tp^{Dur,Me}Fe(1,2\text{-}\eta^2\text{-naphthalene})$ (**8**, top), $Tp^{Dur,Me}Fe(1,2\text{-}\eta^2\text{-anthracene})$ (**9**, middle), and $Tp^{Dur,Me}Fe(1,2\text{-}\eta^2\text{-furan})$ (**10**, bottom). Orange, blue, pink, and gray ellipsoids represent Fe, N, B, and C atoms, respectively. Most hydrogen atoms and co-crystallized solvent molecules are omitted for clarity.

EXPERIMENTAL SECTION

General Considerations. Unless stated otherwise, all compounds were purchased from commercial sources and used without further purification. 2,3,5,6-tetramethylacetophenone was prepared according to a literature procedure.[24] Solvents were dried and deoxygenated by argon sparge followed by passage through an activated alumina column and were stored over 4 Å molecular sieves. All manipulations were performed under an N_2 or argon atmosphere either in a glovebox or using standard Schlenk techniques. ^{1}H NMR spectra were recorded at 298

K using Bruker 400 MHz instruments. Chemical shifts are referenced to residual solvent peaks, IR spectra were recorded using a Bruker Alpha FT-IR with a universal sampling module collecting at 4 cm^{-1} resolution with 32 scans. EPR X-band spectra collected above 100 K were recorded using a Bruker EMX spectrometer and analyzed using Win-EPR software. EPR spectra collected at 15 K were recorded on a Bruker ELEXSYS E500 spectrometer with an Oxford ESR 900 X-band cryostat and a Bruker Cold-Edge Stinger. UV-Vis spectra were recorded using a Cary Bio 500 spectrometer using a 1 cm path length quartz cuvette with a solvent background subtraction applied. X-ray diffraction studies were performed using a Bruker-AXS diffractometer. Elemental Analyses were performed by Midwest Microlabs. Solution phase effective magnetic moments were obtained via the method described by Evans[12] and were performed in triplicate. Standard deviations are reported. The Mössbauer spectrum was recorded on a spectrometer from SEE Co. (formerly WEB Research Co.) operating in the constant acceleration mode in a transmission geometry. The sample was kept in an SVT-300 cryostat from Janis (Wilmington, MA), using liquid N_2 as a cryogen for 80 K measurements. Data analysis was performed using version 4 of the program WMOSS (www.wmoss.org) and quadrupole doublets were fit to Lorentzian lineshapes.[25]

*Synthesis of 1-(2,3,5,6-tetramethylphenyl)butane-1,3-dione (**1**).* A solution of 2,3,5,6-acetophenone (20.0 g, 0.113 mol) in 250 mL of dry THF was refluxed with sodium hydride (6.00 g, 0.250 mol) for 1 hour. The suspension was then cooled to room temperature and ethyl acetate (20.0 mL, 0.203 mol) was added dropwise. Following the addition, the mixture was refluxed again for 6 hours. After cooling to room temperature, the reaction mixture was then quenched with 200 mL water, and then extracted with 200 mL of diethyl ether three times. The aqueous layer was then acidified with 35% hydrochloric acid and extracted again with 200 mL of ether three times. The ether extracts from the acidified aqueous layer were combined, dried over sodium sulfate, and the volatiles removed *in vacuo*. This procedure was repeated three times yielding a combined ~50 g of yellow oil, which was then distilled at 86 °C under vacuum (0.77 mm Hg) to yield a colorless oil which crystallized on cooling to room temperature. Yield: 38 g (51%). ^{1}H NMR (400 MHz, $CDCl_3$) δ 6.98 (s, 1H), 5.61 (s, 1H), 2.22 (s, 6H), 2.16 (s, 3H), 2.15 (s, 6H). ^{13}C NMR (101 MHz, $CDCl_3$) δ 193.6, 189.8, 137.4, 134.1, 132.0, 130.1, 103.1, 25.8, 19.7, 16.3. HRMS (ESI): *m/z* for $C_{14}H_{19}O_2$ $[M+H]^+$ calcd.: 219.1385, found: 219.1375.

*Synthesis of 5-methyl-3-(2,3,5,6-tetramethylphenyl)-1H-pyrazole (**2**).* A solution of **1** (38 g, 0.17 mol) in ethanol (50 mL) was added to a stirring solution of hydrazine monohydrate (10 mL, 0.21 mmol) in 200 mL ethanol, and the resulting solution brought to reflux. After 16 h, the reaction mixture was partitioned between 400 mL of water and 400 mL of ether. The aqueous layer was extracted with 200 mL of ether three times. The combined ether extracts were washed twice with 100 mL of water. The ether extract was subsequently dried over Na_2SO_4, and the volatiles removed *in vacuo*, resulting in a colorless crystalline solid. Yield: 35 g (94 %). ^{1}H NMR (400 MHz, $CDCl_3$) δ 10.79 (br s, 1H), 6.99 (s, 1H), 5.91 (s, 1H), 2.23 (s, 6H), 2.21 (s, 3H), 1.95 (s, 6H). ^{13}C NMR (101 MHz, $CDCl_3$) δ 146.2 (br), 145.4 (br), 133.9, 133.5, 131.6 (br), 131.6, 105.5, 20.0, 16.8, 12.5. HRMS (ESI): *m/z* for $C_{14}H_{19}N_2$ $[M+H]^+$ calcd.: 215.1548, found: 215.1567.

*Synthesis of Sodium bis(5-methyl-3-(2,3,5,6-tetramethylphenyl)-1-pyrazolyl)(3-methyl-5-(2,3,5,6-tetramethylphenyl)-1-pyrazolyl)hydroborate ($NaTp^{Dur,Me}$, **3**).* A hot Schlenk flask was charged with **2** (20.0 g, 93 mmol), evacuated, and then placed under nitrogen. Sodium borohydride (1 g, 26 mmol) was added to the Schlenk flask under a flow of nitrogen. The flask was capped with a glass stopper under a dynamic pressure of N_2 (i.e. an open system) and heated to 80°C and heated to 303°C for 3 hours, with the H2 byproduct venting through the Schlenk sidearm. After being allowed to cool to 60°C, and the viscous oil was triturated with acetonitrile, yielding a pure white solid. Yield: 10 g (56%). ^{1}H NMR (600 MHz, C_6D_6) δ 6.99 (s, 1H), 6.94 (s, 2H), 5.95 (s, 1H), 5.85 (s, 2H), 4.52 (br, 1H), 2.21 (s, 6H), 2.21 – 2.18 (m, 15H), 2.17 (d, 6H), 2.02 (br s, 12H), 1.93 (s, 6H). ^{13}C NMR (151 MHz, C_6D_6) δ 151.0, 149.3, 147.4, 144.6, 137.6, 136.0, 134.4 (br), 134.1, 133.2, 133.0, 131.2, 130.9, 104.9, 104.3, 20.3, 17.3 (br), 17.1, 14.5, 13.1. HRMS (ESI): m/z for $C_{42}H_{54}BN_6$ $[M+2H]^+$ calcd.: 653.4508, found: 653.4644.

*Synthesis of $Tp^{Dur,Me}FeCl$ (**4**).* Under a nitrogen atmosphere, **3** (2.00 g, 2.96 mmol) was dissolved in 80 mL of dry THF and combined with anhydrous $FeCl_2$ (0.420 g, 3.31 mmol). The mixture was stirred for 4 hours, filtered through Celite, and concentrated to 10 mL *in vacuo*. The concentrate was layered with hexanes (20 mL), which precipitated colorless microcrystals. These were collected by filtration and washed with ether (5 mL). Yield: 2.2 g (99%). ^{1}H NMR (400 MHz, C_6D_6) δ (fwhm) 61.31 (35.0 Hz), 58.52 (41.9 Hz), 56.76 (273.7 Hz), 44.97 (45.5 Hz), 11.58 (14.9 Hz), 8.77 (39.3 Hz), 6.47 (15.7 Hz), 6.13 (22.4 Hz), 3.64 (19.1 Hz), 1.46 (24.7 Hz), 1.43 (15.7 Hz), 0.24 (25.7 Hz), −10.18 (157.1 Hz), −28.37 (140.3 Hz), −30.56 (181.4 Hz). Evans Method (C_6D_6): μ_B 5.2 ± 0.2. FTIR: ν_{max} cm^{-1} 2542 (B-H). Calc. for $C_{42}H_{52}BClFeN_6$: C 67.89; H 7.05; N 11.31. Found: C 68.06; H 7.03; N 11.31.

*Synthesis of $(Tp^{Dur,Me}Fe)_2(\mu\text{-}N_2)$ (**5**).* To a solution of **4** (0.500 g, 0.673 mmol) in 50 mL of toluene, potassium graphite (0.300 g, 2.22 mmol) was added. The reaction was monitored by NMR until completion (*ca* 6 hours). The suspension was filtered through celite and the filtrate was concentrated to 20 mL *in vacuo*. Layering the filtrate with hexane (40 mL) provided dark red cubic crystals. Yield: 210 mg (43%). ^{1}H NMR (400 MHz, d_8-THF) δ (fwhm) 78.09 (559.8 Hz), 67.24 (230.4 Hz), 66.70 (205.9 Hz), 54.50 (94.2 Hz), 12.02 (32.5 Hz), 6.89 (25.5 Hz), 5.32 (131.7 Hz), −4.20 (179.5 Hz), −8.84 (59.1 Hz), −9.78 (60.8 Hz), −17.27 (170.7 Hz), −29.15 (262.1 Hz). Evans Method (d_8-THF): μ_B 6.5 ± 0.1. FTIR: ν_{max} cm^{-1} 2540 (B-H). Raman: ν_{max} cm^{-1} 1770 (NN). UV-vis (THF): λ_{max} (nm) (ε_{max} ($M^{-1}cm^{-1}$)) 904 (3.5 x 10^3), 520 (2.9 x 10^3), 436 (3.4 x 10^3). Calc. for $C_{84}H_{104}B_2Fe_2N_{14}$: C 69.91; H 7.26; N 13.59. Found: C 69.81; H 7.51; N 13.71.

*$Tp^{Dur,Me}Fe(C_6H_6)$ (**6**).* Under an argon atmosphere, **5** (80 mg, 0.055 mmol) was dissolved in minimal benzene. The solvent was concentrated *in vacuo* to yield analytically pure black microcrystals. Yield: 87 mg (99%). ^{1}H NMR (400 MHz, C_6D_6) δ (fwhm) 44.30 (21.5 Hz), 38.90 (32.8 Hz), 19.37 (89.6 Hz), 11.18 (9.6 Hz), 9.81 (15.2 Hz), 6.58 (5.7 Hz), 6.11 (17.0 Hz), 5.93 (11.0 Hz), 3.16 (8.7 Hz), 2.67 (5.4 Hz), 1.42 (7.9 Hz), −2.64 (14.89 Hz), −7.56 (63.0 Hz), −10.44 (154.5 Hz). ^{1}H NMR (400 MHz, d_8-THF, argon) δ (fwhm) 130.52 (540.4 Hz), 44.52 (44.9 Hz), 38.68 (54.0 Hz), 19.31 (114.3 Hz), 11.26 (32.3 Hz), 10.00 (38.7 Hz), 7.30 (10.0 Hz), 6.66 (26.0 Hz), 6.06 (41.9 Hz), 6.00 (29.6 Hz), 3.32 (27.8 Hz), 2.78 (27.1 Hz), 0.89 (15.9 Hz),

−2.68 (6.4 Hz), −7.67 (84.6 Hz), −10.98 (167.1 Hz). Evans Method (C_6D_6): μ_B 3.9 ± 0.1. UV-Vis (Benzene) λ_{max} (nm) (ε_{max} ($M^{-1}cm^{-1}$)) 765 (sh, 5.4 x 10^2), 579 (1.3 x 10^3), 384 (sh, 3.2 x 10^3), 301 (sh, 6.4 x 10^3). Calc. for $C_{48}H_{58}BFeN_6$: C 73.38; H 7.44; N 10.70. Found: C 73.09; H 7.29; N 10.45.

*Synthesis of $Tp^{Dur,Me}Fe(3,4\text{-}\eta^2\text{-}PhCF_3)$ (**7**).* Under an argon atmosphere, **5** (50 mg, 0.035 mmol) was dissolved in trifluorotoluene (0.5 mL), producing a deep purple solution. The volatiles were removed *in vacuo* yielding purple glaze that was dissolved in pentane. Slow evaporation afforded crystals suitable for XRD. Yield: 59 mg (99%). ^{1}H NMR (400 MHz, d_8-THF) δ (fwhm) 56.28 (229.2 Hz), 46.68 (24.7 Hz), 39.52 (46.67 Hz), 22.74 (146.3 Hz), 12.26 (21.1 Hz), 12.03 (11.0 Hz), 6.70 (12.7 Hz), 6.58 (26.2 Hz), 6.54 (5.39 Hz), 2.79 (5.13 Hz), −7.27 (81.8 Hz), −13.44 (203.4 Hz). Evans Method (C_6D_6): μ_B 3.9 ± 0.1. UV-Vis (Trifluorotoluene): λ_{max} (nm) (ε_{max} ($M^{-1}cm^{-1}$)) 752 (sh, 5.1 x 10^2), 549 (1.6 x 10^3), 376 (sh, 3.4 x 10^3), 303 (sh, 7.0 x 10^3). Calc. for $C_{49}H_{57}BF_3FeN_6$: C 68.94; H 6.73; N 9.84. Found: C 68.69; H 6.74; N 9.69.

*Synthesis of $Tp^{Dur,Me}Fe(1,2\text{-}\eta^2\text{-}napthalene)$ (**8**). Method 1:* Potassium naphthalenide · 4/3 THF (74 mg, 0.363 mmol) was added to a solution of **4** (170 mg, 0.228 mmol) in toluene (12 mL). The reaction was monitored by NMR until all of the starting material was consumed (~4 hours). The reaction mixture was filtered through celite and concentrated *in vacuo* to 1 mL. Hexanes (4 mL) were added, and the mixture was cooled to −30°C, yielding dark olive-green crystals. Yield: 116 mg (61%). *Method 2:* Solid naphthalene (6 mg, 0.047 mmol) was added to a stirring solution of **5** (25 mg, 0.017 mmol) in toluene (2 mL). The solvent was concentrated *in vacuo* and layered with ether. Cooling to −30 °C overnight produced metallic olive-colored crystals suitable for single-crystal XRD. Yield: 25 mg (86%). ^{1}H NMR (400 MHz, C_6D_6) δ (fwhm) 121.91 (323.1 Hz), 42.53 (30.4 Hz), 34.52 (67.1 Hz), 27.24 (248.6 Hz), 25.81 (273.6 Hz), 12.41 (46.2 Hz), 12.12 (85.8 Hz), 11.12 (19.6 Hz), 8.82 (42.5 Hz), 7.58 (4.1 Hz), 5.48 (13.5 Hz), 3.84 (15.0 Hz), 3.65 (5.3 Hz), −12.27 (102.8 Hz), −18.70 (148.9 Hz). Evans Method (d_8-THF): μ_B 3.7 ± 0.1. UV-vis (THF): λ_{max} (nm) (ε_{max} ($M^{-1}cm^{-1}$)) 921(sh, 1.6 x 10^2), 728 (sh, 3.6 x 10^2), 533 (6.7 x 10^2), 391 (sh, 1.7 x 10^3). Calc. for $C_{48}H_{58}BFeN_6$: C 74.73; H 7.24; N 10.06. Found: C 74.47; H 7.40; N 10.77.

*Synthesis of $Tp^{Dur,Me}Fe(1,2\text{-}\eta^2\text{-}anthracene)$ (**9**).* A stirring solution of **5** (23 mg, 0.016 mmol) in toluene (2 mL) was treated with solid anthracene (8 mg, 0.05 mmol). The solution turned from dark green to dark plum within seconds. The solvent was concentrated to 1 mL *in vacuo* and layered with hexane (2 mL). Cooling to −19°C produced dark purple crystals suitable for single-crystal XRD. Yield: 27 mg (96%). ^{1}H NMR (400 MHz, C_6D_6) δ (fwhm) 139.28 (1036.8 Hz), 52.41 (424.0 Hz), 41.88 (37.3 Hz), 34.59 (78.0 Hz), 21.52 (121.4 Hz), 15.00 (73.8 Hz), 13.81 (61.8 Hz), 10.96 (23.0 Hz), 10.17 (101.8 Hz), 8.83 (50.2 Hz), 7.65 (4.4 Hz), 5.22 (17.7 Hz), 3.86 (5.9 Hz), 3.71 (5.7 Hz), −12.39 (124.8 Hz), −18.33 (207.3 Hz). Evans Method (d_8-THF): μ_B 3.7 ± 0.2. UV-Vis (THF): λ_{max} (nm) (ε_{max} ($M^{-1}cm^{-1}$)) 700 (sh, 1.3 x 10^3), 551 (sh, 2.1 x 10^3), 516 (2.3 x 10^3), 476 (sh, 2.0 x 10^3), 402 (sh, 4.7 x 10^3). Calc. for $C_{56}H_{62}BFeN_6$ (½ × C_6H_{14}): C 76.29; H 7.49; N 9.05. Found: C 76.66; H 7.67; N 9.02.

*Synthesis of $Tp^{Dur,Me}Fe(2,3\text{-}\eta^2\text{-}furan)$ (**10**).* Under an argon atmosphere, **5** (80 mg, 0.055 mmol) was dissolved in furan (1 mL), producing a deep plum color. The solution was concentrated *in vacuo* to ~250 µL and layered with hexane (2 mL). Cooling to −19°C produced dark purple needles, suitable for XRD. Yield: 86 mg (99%). ^{1}H NMR (400 MHz, d_8-THF, argon) δ (fwhm) 59.66 (1552.5 Hz), 47.57 (1507.2 Hz), 36.73 (1311.7 Hz), 30.00 (119.2 Hz), 21.76 (984.9 Hz), 9.52 (753.5 Hz), 7.48 (66.2 Hz), 7.19 (81.8 Hz), 6.36 (90.0 Hz), 0.13 (114.8 Hz), −6.16 (602.6 Hz). Evans Method (d_8-THF): μ_B 3.9 ± 0.1. UV-Vis (THF): λ_{max} (nm) (ε_{max} ($M^{-1}cm^{-1}$)) 800 (p, 5.35 x 10^2), 561 (p, 1.32 x10^3), 371 (sh, 3.18 x 10^3). Due to the high thermal sensitivity of this compound and despite repeated attempts, satisfactory elemental analysis could not be obtained. Spectra are provided in the Supporting Information.

ASSOCIATED CONTENT

Supporting Information

The Supporting Information is available free of charge on the ACS Publications website.

Spectroscopic data and computational details (PDF)

Cartesian coordinates of computed structures (XYZ)

Accession Codes

CCDC 1968324-1968329 contain the supplementary crystallographic data for this paper. This data can obtained free of charge via www.ccdc.cam.ac.uk/data_request/cif or by emailing data_request@ccdc.cam.ac.uk, or by contacting The Cambridge Crystallographic Data Centre, 12 Union Road, Cambridge CB2 1EZ, UK; fax +44 1223 336033.

AUTHOR INFORMATION

Corresponding Author

* E-mail: hill.harman@ucr.edu (W.H.H)

ORCID

Laura A. Essex: 0000-0003-1657-591X

Alex McSkimming: 0000-0000-0000-0000

Niklas B. Thompson: 0000-0003-2745-4945

Margaret L. Kelty: 0000-0000-0000-0000

Ethan A. Hill: 0000-0000-0000-0000

Hill Harman: 0000-0003-0400-2890

Notes

The authors declare no competing financial interest.

ACKNOWLEDGMENT

This research was supported by the National Science Foundation (CHE-1752876) and the American Chemical Society Petroleum Research Fund (57314). NMR spectra were collected on instruments funded by an NSF MRI award (CHE-162673) and an Army Research Office instrumentation grant (W911NF-16-1-0523). W.H.H. is a member of the University of California, Riverside Center for Catalysis. Dr. Fook Tham and Dr. Charlene Tsay are acknowledged for X-ray crystallographic analysis. We also acknowledge Prof. Daniel L. M. Suess for helpful discussions and the use of his Mössbauer spectrometer and Prof. John S. Anderson for the use of his EPR spectrometer.

REFERENCES

[1] a) Muetterties, E. L.; Bleeke, J. R.; Wucherer, E. J.; Albright, T. A. Structural, Stereochemical, and Electronic Features of Arene-Metal Complexes. *Chem. Rev.* **1982**, *82*, 499–525. b) Hubig, S. M.; Lindeman, S. V.; Kochi, J. K. Charge-Transfer Bonding in Metal–Arene Coordination. *Coord. Chem. Rev.* **2000**, *200-202*, 831–873. c) Pampaloni, G. Aromatic Hydrocarbons as Ligands. Recent Advances in the Synthesis, the Reactivity and the Applications of Bis(η^6-arene) Complexes. *Coord. Chem. Rev.* **2010**, *254*, 402–419.

[2] a) Nicholls, B.; Whiting, M. C. 113. the Organic Chemistry of the Transition Elements. Part I. Tricarbonylchromium Derivatives of Aromatic Compounds. *J. Chem. Soc.* **1959**, 551–556. b) Semmelhack, M. F.; Chlenov, A. (Arene)$Cr(CO)_3$ Complexes: Aromatic Nucleophilic Substitution. *Top. Organomet. Chem.* **2004**, *7*, 43–69.

[3] Huttner, G.; Lange, S. Transition metal complexes of cyclic π-ligands. IV. The crystal and molecular structure of bis(hexamethylbenzene)ruthenium(0), a complex containing a bent tetrahapto benzene nucleus. *Acta Crystallagr., Sect. B* **1972**, *B28*, 2049–2060.

[4] a) Krueger, D. J. B. C. Bonding of Aromatic Hydrocarbons to Nickel(0). Structure of Bis(Tricyclohexylphosphine)(1,2-η^2-Anthracene)Nickel(0)-Toluene. **2015**, 1–8. b) Harman, W. D.; Taube, H. Reactivity of Pentaammineosmium(II) with Benzene. *J. Am. Chem. Soc.* **1987**, *109*, 1883–1885. c) Meiere, S. H.; Brooks, B. C.; Gunnoe, T. B.; Sabat, M.; Harman, W. D. A Promising New Dearomatization Agent: Crystal Structure, Synthesis, and Exchange Reactions of the Versatile Complex TpRe(CO)(1-methylimidazole)(η^2-benzene) (Tp = Hydridotris(Pyrazolyl)Borate). Organometallics 2001, 20, 1038–1040. d) Graham, P. M.; Meiere, S. H.; Sabat, M.; Harman, W. D. Dearomatization of Benzene, Deamidization of N, N-Dimethylformamide, and a Versatile New Tungsten π-Base. *Organometallics* **2003**, *22*, 4364–4366. e) Margulieux, G. W.; Bezdek, M. J.; Turner, Z. R.; Chirik, P. J. *J. Am. Chem. Soc.* **2017**, *139*, 6110–6113.

[5] a) Harman, W. D. The Activation of Aromatic Molecules with Pentaammineosmium(II). *Chem. Rev*. **1997**, 1–26. b) Liebov, B. K.; Harman, W. D. Group 6 Dihapto-Coordinate Dearomatization Agents for Organic Synthesis. *Chem. Rev.* **2017**, *117*, 13721–13755.

[6] Trofimenko, S. Recent Advances in Poly(pyrazolyl)borate (Scorpionate) Chemistry. *Chem. Rev.* **1993**, *93*, 943–980.

[7] a) McSkimming, A.; Harman, W. H. A Terminal N_2 Complex of High-Spin Iron(I) in a Weak, Trigonal Ligand Field. *J. Am. Chem. Soc.* **2015**, *137*, 8940–8943. b) Cummins, D. C.; Yap, G. P. A.; Theopold, K. H. Scorpionates of the "Tetrahedral Enforcer" Variety as Ancillary Ligands for Dinitrogen Complexes of First Row Transition Metals (Cr-Co). *Eur. J. Inorg. Chem.* **2016**, 2349–2356.

[8] Kisko, J. L.; Hascall, T.; Parkin, G. The Synthesis, Structure, and Reactivity of Phenyl Tris(3-tert-butylpyrazolyl)borato Iron Methyl, [$PhTp^{tBu}$]FeMe: Isolation of a Four-Coordinate Monovalent Iron Carbonyl Complex, [$PhTp^{tBu}$]FeCO. *J. Am. Chem. Soc.* **1998**, *120*, 10561–10562.

[9] a) Shirasawa, N.; Akita, M.; Hikichi, S.; Moro-oka, Y. Thermally Stable Coordinatively Unsaturated Alkyl Complexes Resistant to β-Hydride Elimination: $Tp^{iPr}M–CH_2CH_3$ (M = Co, Fe). *Chem. Commun.* **1999**, 417–418. b) Brunker, T. J.; Hascall, T.; Cowley, A. R.; Rees, L. H.; O'Hare, D. Variable Coordination Modes of Hydrotris(3-Isopropyl-4-Bromopyrazolyl)Borate (Tp') in Fe(II), Mn(II), Cr(II), and Cr(III) Complexes: Formation of MTp'Cl (M = Fe and Mn), Structural Isomerism in $CrTp'_2$, and the Observation of Tp'^- as an Uncoordinated Anion. *Inorg. Chem.* **2001**, *40*, 3170–3176. c) Shirasawa, N.; Nguyet, T. T.; Hikichi, S.; Moro-oka, Y.; Akita, M. Tetrahedral, Highly Coordinatively Unsaturated 14 e^- (Fe) and 15 e^- (Co) Hydrocarbyl Complexes Bearing Hydrotris(pyrazolyl)borato Ligands ($Tp^{R'}$), $Tp^{R'}M–R$ (M = Fe, Co, Ni). *Organometallics* **2001**, *20*, 3582–3598. d) Jové, F. A.; Pariya, C.; Scoblete, M.; Yap, G. P. A.; Theopold, K. H. A Family of Four-Coordinate Iron(II) Complexes Bearing the Sterically Hindered Tris(pyrazolyl)borato Ligand $Tp^{tBu,Me}$. *Chem. Eur. J.* **2011**, *17*, 1310–1318.

[10] a)Rheingold, A. L.; White, C. B.; Trofimenko, S. Hydrotris(3-mesitylpyrazol-1-yl)borate and Hydrobis(3-mesitylpyrazol-1-yl)(5-Mesitylpyrazol-1-yl)Borate: Symmetric and Asymmetric Ligands with Rotationally Restricted Aryl Substituents. *Inorg. Chem.* **1993**, *32*, 3471–3477. b) Yap, G. P. A.; Jove, F.; Urbano, J.; Alvarez, E.; Trofimenko, S.; Díaz-Requejo, M. M.; Pérez, P. J. Unusual Polybrominated Polypyrazolylborates and Their Copper(I) Complexes: Synthesis, Characterization, and Catalytic Activity. *Inorg. Chem.* **2007**, *46*, 780–787. c) van Dijkman, T. F.; Siegler, M. A.; Bouwman, E. Highly Tunable Fluorinated Trispyrazolylborates $[HB(3\text{-}CF_3\text{-}5\text{-}\{4\text{-}RPh\}pz)_3]^-$ (R = NO_2, CF_3, Cl, F, H, OMe and NMe_2) and Their Copper(I) Complexes. *Dalt. Trans.* **2015**, *44*, 21109–21123.

[11] Smith, J. M.; Sadique, A. R.; Cundari, T. R.; Rodgers, K. R.; Lukat-Rodgers, G.; Lachicotte, R. J.; Flaschenriem, C. J.; Vela, J.; Holland, P. L. Studies of Low-Coordinate Iron Dinitrogen Complexes. *J. Am. Chem. Soc.* **2006**, *128*, 756–769.

[12] a) Evans, D. F. 400. the Determination of the Paramagnetic Susceptibility of Substances in Solution by Nuclear Magnetic Resonance. *J. Chem. Soc.* **1959**, 2003–2003. b) Schubert, E. M. Utilizing the Evans Method with a Superconducting NMR Spectrometer in the Undergraduate Laboratory. *J. Chem. Educ.* **1992**, *69*, 62.

[13] Welch, K. D.; Harrison, D. P.; Lis, E. C.; Liu, W.; Salomon, R. J.; Harman, W. D.; Myers, W. H. Large-Scale Syntheses of Several Synthons to the Dearomatization Agent {$TpW(NO)(PMe_3)$} and Convenient Spectroscopic Tools for Product Analysis. *Organometallics* **2007**, *26*, 2791–2794.

[14] Myers, J. T.; Smith, J. A.; Dakermanji, S. J.; Wilde, J. H.; Wilson, K. B.; Shivokevich, P. J.; Harman, W. D. Molybdenum(0) Dihapto-Coordination of Benzene and Trifluorotoluene: the Stabilizing and Chemo-Directing Influence of a CF_3 Group. *J. Am. Chem. Soc.* **2017**, *139*, 11392–11400.

[15] Six structures were found in the Cambridge Structural Database containing well-ordered molecules of free $PhCF_3$ (Version 5.41, March 2020). Among these, the C–C bonds ranged from 1.36 to 1.40 Å, with average C_{ipso}–C_{ortho}, C_{ortho}-C_{meta}, and C_{meta}-C_{para} distances of 1.384(9), 1.382(10), and 1.382(9), respectively. Numbers in parentheses are standard deviations.

[16] Hagen, W. R. EPR Spectroscopy of Iron–Sulfur Proteins. *Adv. Inorg. Chem.* **1992**, *38*, 165–222.

[17] a) Reger, D. L.; Gardinier, J. R.; Elgin, J. D.; Smith, M. D.; Hautot, D.; Long, G. J.; Grandjean, F. Structure−Function Correlations in Iron(II) Tris(pyrazolyl)borate Spin-State Crossover Complexes. *Inorg. Chem.* **2006**, *45*, 8862–8875. b) McWilliams, S. F.; Brennan-Wydra, E.; MacLeod, K. C.; Holland, P. L. Density Functional Calculations for Prediction of ^{57}Fe Mössbauer Isomer Shifts and Quadrupole Splittings in β-Diketiminate Complexes. *ACS Omega* **2017**, *2*, 2594–2606.

[18] Zhao, Y.; Truhlar, D. G. A New Local Density Functional for Main-Group Thermochemistry, Transition Metal Bonding, Thermochemical Kinetics, and Noncovalent Interactions. *J. Chem. Phys.* **2006**, *125*, 194101–194119.

[19] Weigend, F.; Ahlrichs, R. Balanced Basis Sets of Split Valence, Triple Zeta Valence and Quadruple Zeta Valence Quality for H to Rn: Design and Assessment of Accuracy. *Phys. Chem. Chem. Phys.* **2005**, *7*, 3297–3305.

[20] Neese, F. Orca 4.2.1. *Wiley Interdiscip. Rev. Comput. Mol. Sci.* **2012**, 2, 73.

[21] a) Hoyt, J. M.; Sylvester, K. T.; Semproni, S. P.; Chirik, P. J. Synthesis and Electronic Structure of Bis(imino)pyridine Iron Metallacyclic Intermediates in Iron-Catalyzed Cyclization Reactions. *J. Am. Chem. Soc.* **2013**, *135*, 4862–4877. b)Joannou, M. V.; Darmon, J. M.; Bezdek, M. J.; Chirik, P. J. Exploring C(sp3)–C(sp3) reductive elimination from an isolable iron metallacycle. *Polyhedron* **2019**, *159*, 308–317.

[22] a) Chen, H.; Hodges, L. M.; Liu, R.; Stevens, W. C. J.; Sabat, M.; Harman, W. D. Dearomatization of Furan: Structure of an η^2-Furan Complex and a Survey of Its Reactivity. *J. Am. Chem. Soc.* **1994**, *116*, 5499–5500. b) Meiere, S. H.; Brooks, B. C.; Gunnoe, T. B.; Carrig, E. H.; Sabat, M.; Harman, W. D. Dihapto Coordination of Aromatic Molecules by the Asymmetric π-Bases {TpRe(CO)(L)} (Tp = Hydridotris(pyrazolyl)borate; L = tBuNC, PMe_3, Pyridine, 1-Methylimidazole, or NH_3). *Organometallics* **2001**, *20*, 3661–3671.

[23] a) Hamon, J.-R.; Astruc, D.; Michaud, P. Syntheses, Characterizations, and Stereoelectronic Stabilization of Organometallic Electron Reservoirs: the 19-Electron d^7 Redox Catalysts η^5-C_5R_5Fe-η^6-$C_6R'_6$. *J. Am. Chem. Soc.* **1981**, *103*, 758–766. b) Hickey, A. K.; Lee, W.-T.; Chen, C.-H.; Pink, M.; Smith, J. M. A Bidentate Carbene Ligand Stabilizes a Low-Coordinate Iron(0) Carbonyl Complex. *Organometallics* **2016**, *35*, 3069–3073.

[24] Ahdreou, A. D.; Bulbulian, R. V.; Gore, P. H. Friedel-Crafts Acetylation of Durene, Isodurene and Prehnitene. *Tetrahedron* **1980**, *36*, 2101–2104.

[25] Prisecaru, VMOSS4 Mössbauer Spectral Analysis Software, www.vmoss.org, 2009-2016.

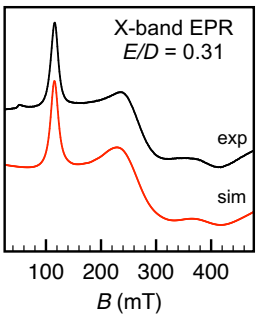

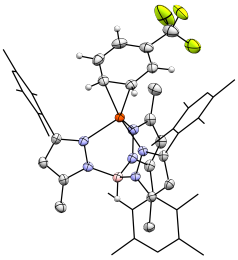

TpFe(I)(η^2-PhCF$_3$)
S* = *3/2